

# Titrations without the additions: The efficient determination of $pK_a$ values using NMR imaging techniques

Matthew Wallace,<sup>\*,†,‡</sup> Dave J. Adams,<sup>†,#</sup> and Jonathan A. Iggo<sup>\*,†</sup>

<sup>†</sup>Department of Chemistry, University of Liverpool, Crown Street, Liverpool, L69 7ZD, UK

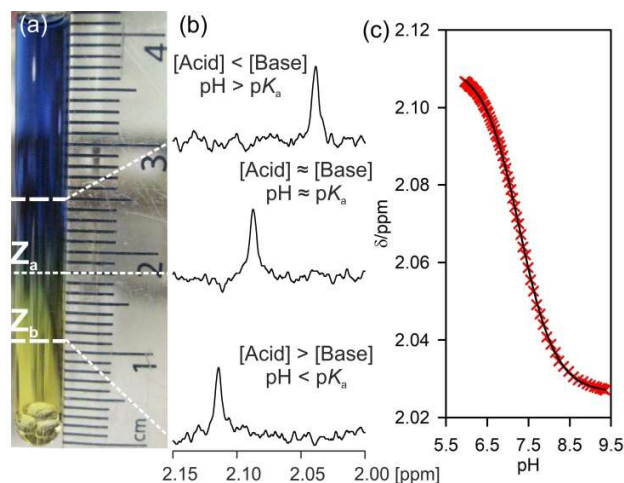
<sup>‡</sup>School of Pharmacy, University of East Anglia, Norwich Research Park, Norwich, NR4 7TJ, UK

**ABSTRACT:** It can be very informative to acquire NMR spectra of a sample as a function of the solution pH. Examples can be found in the design of host-guest complexes or in the determination of the  $pK_a$  values of organic molecules. In the conventional procedure, a series of spectra must be recorded and the pH of the sample adjusted manually between successive NMR measurements. As an alternative to this laborious procedure, we demonstrate how controlled pH gradients may be established in 5 mm NMR tubes and analysed using standard NMR equipment in a “single shot” experiment. Using  $^1\text{H}$  NMR imaging techniques and a set of NMR pH indicator compounds, we are able to measure the pH of a sample as a function of position along a pH gradient. We are thus able to obtain the necessary set of  $^1\text{H}$  NMR spectra as a function of pH from a single sample in a single NMR experiment. As proof of concept, we demonstrate how the technique may be employed for the determination of the  $pK_a$  values of small organic molecules. We are able to measure  $pK_a$  values from 1-11 to within 0.1 units of their literature values. The method is robust to variations in the setting of the pH gradients and can be readily implemented through an automated sample changer.

The pH of a solution is a fundamental parameter which determines the chemical and biological activity of the species within.<sup>1-3</sup> For example, the conformation and activity of a protein can change significantly with the solution pH.<sup>4,5</sup> Elsewhere, the pH is of great importance when designing host-guest systems<sup>6</sup> and self-assembled materials.<sup>7-9</sup> In such systems, it can be useful to acquire  $^1\text{H}$  NMR spectra of a sample as a function of the solution pH. The chemical shifts of moieties participating in chemical phenomena such as protonation/deprotonation,<sup>10-13</sup> host-guest complexation<sup>14-16</sup> or supra-molecular assembly<sup>17-19</sup> are often observed to vary with pH. Valuable information including  $pK_a$  values,<sup>12,20-22</sup> conformations<sup>5,23,24</sup> and assembly states<sup>18,19</sup> can thus be obtained by analysis of chemical shift data. In the conventional procedure, a series of NMR spectra are recorded separately, the pH of the sample being adjusted manually between successive NMR measurements. This procedure is extremely demanding in terms of labour, sample volume and instrument time; either a multitude of samples must be prepared and measured or a single sample repeatedly inserted into the spectrometer, a spectrum recorded, the sample removed, the pH adjusted and the sample reinserted into the spectrometer.

A more efficient procedure would be to establish a pH gradient across a single sample and record spatially resolved spectra along the length of the gradient using chemical shift imaging (CSI) techniques. In this way, it would be possible to acquire a complete series of spectra as a function of pH in a single NMR experiment.<sup>25-27</sup> Herein, we demonstrate how controlled pH gradients may be established in 5 mm NMR tubes and analysed using standard NMR equipment to obtain the  $pK_a$  of an analyte. We present a series of indicator molecules that permit the determination of the pH as a function of position along a sample using CSI techniques. As proof of concept, we demonstrate the accurate determination of the  $pK_a$

values of small organic molecules (Scheme 1). By comparison of  $pK_a$  values obtained here with literature data, we are able to verify our methods for the controlled establishment and analysis of pH gradients as well as the validity and precision of the method for  $pK_a$  determination.



**Scheme 1.** A pH gradient is established in a 5 mm NMR tube (a).  $^1\text{H}$  NMR spectra are recorded along the length of the gradient (b) within the NMR-active region of the sample (between thick white lines). The  $^1\text{H}$  chemical shift of an analyte, bromothymol blue, can then be measured as a function of pH and a  $pK_a$  value extracted (c). The black line is the fit to Equation 1. Positions  $Z_a$  and  $Z_b$  are used in the calculation of the parameters for the establishment of the optimum pH gradient (*vide infra*).

The use of NMR spectroscopy to determine the  $pK_a$  values of molecules is well-established and is discussed extensively elsewhere.<sup>10,12,21</sup> Briefly, the chemical shift of an analyte mol-

ecule,  $\delta_{\text{obs}}$ , is recorded as a function of the solution pH. The  $pK_a$  can then be determined by fitting the data to Equation 1:

$$\delta_{\text{obs}} = \frac{\delta_{\text{H}}10^{(pK_a - \text{pH})} + \delta_{\text{L}}}{1 + 10^{(pK_a - \text{pH})}} \quad (1)$$

where  $\delta_{\text{H}}$  and  $\delta_{\text{L}}$  are the limiting chemical shifts of the totally protonated and deprotonated analyte species respectively. The ability to measure the pH directly by  $^1\text{H}$  NMR in a localised manner is essential in the present work. Where the  $pK_a$  of a compound is known, Equation 1 can be rearranged to yield the pH of the solution:

$$\text{pH} = pK_a + \log_{10} \left( \frac{\delta_{\text{obs}} - \delta_{\text{H}}}{\delta_{\text{L}} - \delta_{\text{obs}}} \right) \quad (2)$$

By combining a number of NMR indicator compounds spanning a range of  $pK_a$  values, it is possible to determine the pH of a solution over a wide range with good accuracy.<sup>17,20,21,28-31</sup>

## EXPERIMENTAL SECTION

**Materials.** All chemicals were purchased from Sigma-Aldrich and used as received. Oxalic acid was purchased as the dihydrate. Monosodium malonate was prepared by the addition of one mole equivalent of NaOH to an aqueous solution of malonic acid followed by removal of the water *in vacuo*. The number of moles of malonate per gram of product was measured by  $^1\text{H}$  NMR by integration of the malonate  $\text{CH}_2$  resonance against an internal standard capillary. The molecular weight of the product was obtained as 125.8 g/mol, in good agreement with the theoretical mass of 126.06 g/mol for anhydrous monosodium malonate. The pH of a 43 mM aqueous solution of the product was measured as 4.13, in good agreement with a value of 4.12 calculated using the CurTiPot package.<sup>32</sup>

**Preparation of Samples.** Stock solutions of the NMR indicator Sets A and B (Table 1, Results and Discussion Section) were prepared and used throughout the study. These solutions were 0.2 M in each indicator, with the exception of formate and 2,6-lutidine which were included at 0.4 M and 0.1 M respectively. Methylamine was included as the hydrochloride salt with one mole equivalent of NaOH added. A stock solution of the NMR reference compounds was prepared containing sodium methanesulfonate (0.1 M), 2,2-dimethyl-2-silapentane-5-sulfonate (DSS, 20 mM) and 1,4-dioxane (1 vol%). The analyte molecules tested comprised 2,6-dihydroxybenzoic acid, *L*-tyrosine, 3,5-dinitrobenzoic acid, glycolic acid, propionic acid, benzimidazole, bromothymol blue, 4-cyanophenol, benzylamine, 2,6-dimethylphenol and *tert*-butylamine. Solutions of the analytes were prepared separately in MilliQ water at a standard concentration of 2 mM. Due to solubility limitations, bromothymol blue was analysed at a concentration of 0.1 mM. Where analytes were included in their protonated form, one mole equivalent of NaOH was added. The 2,6-dimethylphenol and *tert*-butylamine samples contained 10 mM NaOH in addition to the analytes and indicators to ensure the alkaline half of the titration curve could be adequately sampled. The NMR indicator and reference compounds were included at a 1:100 dilution of their concentration in the stock solutions.

All experiments were performed in 5 mm Norell 502 NMR tubes. To establish a pH gradient, solid acid was weighed into the tube using a Mettler AE101 balance with a stated precision of  $\pm 0.01$  mg. Weighings of 0.6 mg on this balance were found

by NMR to be within 20% of their nominal value, from three repeat measurements. Four 2 mm diameter glass beads (Assistent, Germany) were then placed on top of the acid. Prior to use, the beads were washed with analytical grade methanol and dried. An aliquot of the analyte solution was drawn up in a 9'' Pasteur pipette and gently layered on top of the glass beads to a height of 40 mm from the base of the NMR tube. The glass beads served to prevent excessive mixing of the acid and the analyte solution. The samples were then left to stand in a water bath at 25 °C until analysis. When HCl was used as a diffusant, an aqueous solution (2 M, 30  $\mu\text{L}$ ) was carefully measured into the NMR tube and six glass beads placed in the solution. A list of the parameters used in each titration is provided in Table 4. In all cases,  $h$  (Equation 5) was taken as 2 mm and  $r$  (Equation 8) as 2.1 mm.  $Z_a$  and  $Z_b$  (Equation 6) were determined as 18 mm and 11 mm above the base of the NMR tube respectively (Scheme 1, a). These values were obtained by the analysis of a biphasic sample by CSI (Section 1, Supporting Information). This sample comprised a 1 M solution of NaCl in 10%  $\text{H}_2\text{O}/90\%$   $\text{D}_2\text{O}$  layered on top of a solution of 10%  $\text{CHCl}_3$  in  $\text{CDCl}_3$ . Spectra obtained within  $\pm 7$  mm from the centre ( $Z_a$ ) of the NMR-active region were used to calculate the analyte  $pK_a$  values. Beyond this region, the quality of the spectra obtained deteriorate rapidly with distance from the coil centre.

For the determination of the indicator  $pK_a$  values (Table 2), the NMR indicators and reference compounds were included in the buffer solutions at a 1:2000 dilution in order to minimise the effect of the indicators on the buffer pH. The pH and ionic strength of each buffer is quoted in Table 2 as the value at 25 °C predicted using the CurTiPot package.<sup>32</sup> The pH of each buffer was checked using a Hanna Instruments HI-8424 meter equipped with an FC200 probe. In all cases, the measured pH of the buffers agreed with the theoretical value within a sensible error of our meter ( $\pm 0.03$  units).<sup>28</sup> The buffer systems used comprised HCl, citrate, phosphate and carbonate. The composition of the buffer solutions, theoretical pH values and measured pH values are provided in Table S-4 in the Supporting Information. Prior to use, the pH meter was freshly calibrated with pH 7.01 and 10.01 or 4.01 buffer solutions (Hanna Instruments).

**NMR.** Experiments were performed on a Bruker Avance II 400 MHz wide bore spectrometer operating at 400.20 MHz for  $^1\text{H}$ . The probe was equipped with Z-axis pulsed field gradients. The temperature of the samples was maintained at  $298 \pm 0.5$  K, the variation in the temperature with time being less than 0.1 K. CSI experiments were performed using a gradient phase encoding sequence based on that of Trigo-Mouriño *et al.*<sup>33</sup> and incorporating the double echo hard-pulse WATERGATE (W) sequence of Liu *et al.*<sup>34</sup> (Bruker library ZGGPW5) to suppress the  $\text{H}_2\text{O}$  resonance. The pulse sequence was thus  $W-\tau_1-g-\tau_2$ -acquire where  $g$  is a gradient pulse and  $\tau_1$  and  $\tau_2$  are delays of 10  $\mu\text{s}$  and 200  $\mu\text{s}$  respectively. A spoil gradient (27 G/cm) was employed at the end of the signal acquisition period (1 s) to destroy any transverse magnetisation. The gradient pulse was 242  $\mu\text{s}$  in duration and varied between -27 and 27 G/cm in 128 steps. The shape of the pulse was a smoothed square. 8 scans were acquired at each step giving a total acquisition time of 20 minutes and a theoretical spatial resolution of 0.20 mm. 16 dummy scans were acquired prior to signal acquisition. The delay between successive hard pulses in the selective pulse train was set at 250  $\mu\text{s}$  corresponding to a

4000 Hz separation between the null points of the W sequence. When resonances of interest occur close to the water resonance, for example with glycolic acid and benzylamine as analytes, a double-echo excitation sculpting (ES) sequence was found to give superior signal quality. However, both sequences gave identical  $pK_a$  values within error (Section 8, Supporting Information). This sequence was based on the Bruker sequence, ZGESGP, with the encoding gradient pulse within the last spin-echo of the sequence. Spectra were recorded with 12 scans at each gradient increment, otherwise using the same parameters as the W sequence. Gaussian pulses of 4 ms duration and 300 Hz peak power were applied to selectively suppress the H<sub>2</sub>O resonance. The W sequence was used as standard in this work as it gave superior water suppression.

DSS was used as the reference for all spectra (0 ppm). The other reference compounds listed in Table 1 give equivalent results (Figure S-2, Supporting Information). No D<sub>2</sub>O was included in the samples in order to allow the direct comparison of the analyte  $pK_a$  values measured in this work with literature data.<sup>35</sup> All measurements were thus performed off-lock. NMR data was processed in Bruker TopSpin 3.2. CSI images were processed in phase-sensitive mode following the procedure of Trigo-Mouriño *et al.*<sup>33</sup> Following two-dimensional Fourier transformation of the CSI datasets, the individual spectra were automatically extracted, any residual phase errors corrected and the spectra referenced to DSS (0 ppm) using an automation macro written in house. Analyte and indicator chemical shift data were imported from TopSpin into Microsoft Excel and analysed to obtain solution pH as a function of position. Non-linear fitting of this data to Equation 1 to obtain the analyte  $pK_a$  was accomplished using the procedure of Brown.<sup>36</sup> The limiting analyte chemical shifts were treated as free parameters in the fitting. The fitted limiting chemical shifts were in excellent agreement with those measured by manually adjusting the pH of a sample to the extreme pH values of the titration curves. Employing the measured limiting shifts in the fitting did not significantly change the analyte  $pK_a$  values obtained (Section 3, Supporting Information).

## RESULTS AND DISCUSSION

**Determination of pH by <sup>1</sup>H NMR.** The NMR pH indicators used in this work are listed in Table 1 along with the compounds used to provide reference chemical shifts. These indicators allow accurate pH determinations over the range 1-12. In the present work, it is not necessary to be able to measure over this full range in a single sample. The indicators used are therefore divided into two sets in order to avoid redundancy and minimise spectral overlap between the indicators and other compounds of interest. Set A can be used for weakly alkaline and acidic measurements while Set B is used exclusively for alkaline measurements. The limiting chemical shifts of the indicators were measured following the procedure described in Section 4 of the Supporting Information.<sup>17</sup> Calibration curves are also provided.

**Table 1. NMR pH indicators used in this work.<sup>a</sup>**

pH range	Indicator <sup>a</sup>
1-10 (Set A)	Dichloroacetate <sup>b</sup> (DCA), formate, acetate, 2,6-lutidine, glycinate, methylphosphonate (MPA <sup>2-</sup> )
8-12 (Set B)	MPA <sup>2-</sup> , glycinate, methylamine
Reference	1,4-Dioxane, 2,2-dimethyl-2-silapentane-5-sulfonate (DSS), methanesulfonate

<sup>a</sup>Anions were included as their Na<sup>+</sup> salts in all cases. <sup>b</sup>DCA was included only for very acidic (pH < 2) measurements.

In order to determine the  $pK_a$  values of the indicators, the chemical shifts of the indicators were measured in a series of buffer solutions (Table 2). The  $pK_a$  values of the indicators were then extracted using Equation 2. It is important to note that the  $pK_a$  values listed in Table 2 are the ‘effective’  $pK_a$  values of the indicators,<sup>37,38</sup> defined as:

$$pK_a = -\log_{10} \frac{a_{H^+} [A]}{[HA]} \quad (3)$$

where  $a_{H^+}$  denotes the activity of H<sup>+</sup> and [A] and [HA] are the concentrations of the deprotonated and protonated forms of the indicator respectively. When used with Equation 2, the indicator parameters given in Table 2 thus yield the activity-based pH. In all experiments discussed in this paper, the ionic strength does not exceed the strengths of the calibration buffers by more than 0.1 units (Table S-4, Supporting Information). The variation of the indicator  $pK_a$  values with ionic strength, and therefore the pH values determined, will be no more than 0.1 units within these ranges.<sup>39,46</sup> The limiting chemical shifts of indicators can be assumed independent of ionic strength.<sup>28,35</sup> Correcting the indicator  $pK_a$  values for the variation of ionic strength during titrations did not significantly improve the accuracy of the analyte  $pK_a$  values (Section 11, Supporting Information).

The sensitivity, S, of an indicator to the pH of the solution can be defined as the first derivative of the indicator chemical shift with respect to pH.<sup>10,28</sup> S can thus be obtained from Equation 2 as:

$$S = (\ln 10) \left[ \frac{(\delta_L - \delta_{obs})(\delta_{obs} - \delta_H)}{\delta_H - \delta_L} \right] \quad (4)$$

To calculate the pH of a solution, the indicators were grouped into pairs: DCA/MPAH<sup>-</sup>, MPAH<sup>-</sup>/formate, formate/acetate, acetate/lutidine, lutidine/MPA<sup>2-</sup>, MPA<sup>2-</sup>/glycinate and glycinate/methylamine. S was calculated for each indicator and the pair with the greatest combined sensitivity selected. The apparent pH of the solution was calculated for each indicator using Equation 2. The pH of the solution could then be obtained as the average of the apparent pH values reported by each indicator in the pair, weighted by S.

**Table 2.  $pK_a$  values and limiting chemical shifts of NMR indicators used in this work.<sup>a</sup>**

Indicator	$pK_a$	$\delta_i$ /ppm	$\delta_H$ /ppm	Buffer pH (Ionic strength/mM)
DCA	1.21( $\pm 0.004$ )	6.0480	6.3118	1.11 (100), 1.78 (20),
MPAH <sup>-</sup>	2.32( $\pm 0.004$ )	1.2819	1.5106	1.78 (20), 3.15 (12),
Formate	3.63( $\pm 0.04$ )	8.4414	8.2669	3.15 (12), 4.55 (42)
Acetate	4.63	1.9060	2.0830	4.55 (42)
2,6-lutidine	6.87	2.4563	2.7074	6.98 (41)
MPA <sup>2-</sup>	7.75	1.0711	1.2819	6.98 (41)
Glycinate	9.74	3.1754	3.5494	10.09 (41)
Methylamine	10.79	2.2901	2.5942	10.09 (41)

<sup>a</sup>The  $pK_a$  values quoted apply to the protonated indicator species. The calibration buffers and ionic strengths are also provided. Where two calibration buffers are used, the average  $pK_a$  value is quoted  $\pm$  half the difference between the measured values.

**Establishment of the optimum pH gradient.** To establish a pH gradient in a 5 mm NMR tube, crystals of a solid acid are placed at the base of the tube and an alkaline solution of the analyte and pH indicators placed on top using a pipette. Dissolution and diffusion of the acid up the NMR tube then establishes the pH gradient. By recording spatially resolved <sup>1</sup>H spectra along the length of the pH gradient, it is possible to measure the pH as a function of position using the indicator compounds. The chemical shift of the analyte can thus be measured as a function of pH and a  $pK_a$  value extracted using Equation 1 (Scheme 1, c).

The reliable determination of a  $pK_a$  value requires the establishment of a smooth pH gradient spanning ca. 2-3 units around the expected  $pK_a$  of the analyte. Such gradients can readily be established by selecting a monoprotic acid with a  $pK_a$  equal to, or not more than one unit below, the expected  $pK_a$  of the analyte. Buffering by the acid will give the desired smooth pH gradient while the presence of an excess of the acid towards the lower part of the tube will not cause the pH to fall more than ca. 1-2 units below the  $pK_a$  of the analyte. The acidic diffusants used in this work are listed in Table 3 along with the approximate range spanned by the resulting pH gradient. In addition to monoprotic acids, diprotic acids can be used where the expected  $pK_a$  of the analyte straddles those of the acid.

**Table 3. Acidic diffusants used in this work.**

Acid diffusant <sup>a</sup>	pH range <sup>b</sup>
HCl (-6)	1-3
Oxalic acid (1.3, 3.8)	1.5-4.5
Glycolic acid (3.8)	3-6
Malonic acid (2.9, 5.7)	3-6
Monosodium malonate (NaMal, 5.7)	4.5-9
KH <sub>2</sub> PO <sub>4</sub> (7.2)	6-10
B(OH) <sub>3</sub> (9.3)	8-11
NaHCO <sub>3</sub> (10.3)	9-12

<sup>a</sup>The  $pK_a$  values of the acids are given in parentheses and are taken from Reference <sup>47</sup>. <sup>b</sup>The usable pH range spanned by the resulting gradients.

The calculation of the mass of diprotic acid required for the establishment of the optimum pH gradient differs slightly from the monoprotic case (Section 5, Supporting Information). We note that data from separate samples can be readily combined to span much larger pH ranges, if required (Section 6, Supporting Information).

When performing a titration, the mass of monoprotic acid required and the time at which the optimum pH gradient will be established can be calculated as follows: The acids used in this work are highly water soluble and dissolve within minutes of placing the analyte solution on top. Mathematically, the acid behaves as though it were diffusing from a plane source at the base of the NMR tube. The concentration,  $C_z$ , of diffusing acid at a height  $Z$  from the base of the NMR tube after a time,  $t$ , is therefore given by Equation 5:<sup>48</sup>

$$C_z = N_{(t)} \exp\left(-\frac{(Z-h)^2}{4Dt}\right) \quad (5)$$

where  $D$  is the diffusion coefficient of the acid and  $N_{(t)}$  is a time dependent parameter.  $h$  is the thickness of the solid acid when placed at the base of the NMR tube. A pH gradient can be defined in terms of the number of equivalents of diffusing acid to base at heights  $Z_a$  and  $Z_b$  (Scheme 1, a). From Equation 5, such a gradient will have become established at a unique time,  $t_{opt}$ , given by Equation 6:

$$t_{opt} = \frac{(Z_b - h)^2 - (Z_a - h)^2}{4D \ln\left(\frac{\alpha}{\beta}\right)} \quad (6)$$

where  $\alpha$  and  $\beta$  denote the number of equivalents of diffusing acid to basic species at heights  $Z_a$  and  $Z_b$  respectively. At the lower limit of the NMR-active region ( $Z_b$ ), it is necessary to have an excess of acid relative to base so that the acidic region of the titration curve may be sampled. In the following discussion, it is assumed that the initial concentration of base is constant throughout the analyte solution. Diffusion of basic species down the sample towards the acid is ignored. Fixing the initial concentration of basic species as  $C_o$ ,  $N_{(t)}$  may be obtained from Equation 5 as:

$$N_{(t)} = \alpha C_o \exp\left(\frac{(Z_a - h)^2}{4Dt_{opt}}\right) \quad (7)$$

Only basic species whose  $pK_a$  value when protonated,  $pK_{aH}$ , is greater than one unit below the  $pK_a$  of the diffusing acid are included in the summation of  $C_o$ . Basic species with smaller  $pK_{aH}$  values will be unable to deprotonate the diffusing acid. When using acid diffusants which are strong relative to the analyte ( $pK_{a,acid} < pK_{a,analyte} - 0.5$ ), only half an equivalent of acid is included relative to the analyte in the summation of  $C_o$ . Basic species with  $pK_{aH}$  values smaller than the  $pK_a$  of such acids are discounted from the summation of  $C_o$ . The mass of acid,  $m$ , required can be obtained by integration of Equation 5 over the length of the sample and is thus given by Equation 8:

$$m = \pi r^2 \alpha C_o M_r \sqrt{\pi D t_{opt}} \exp\left(\frac{(Z_a - h)^2}{4 D t_{opt}}\right) \quad (8)$$

where  $r$  is the radius of the NMR tube and  $M_r$  the molecular weight of the acid. Diffusion coefficients for acids listed in Table 3 are provided in Section 7, Supporting Information.

As an example calculation, a 2 mM solution of 2,6-dimethylphenol was prepared containing 12 mM NaOH and 2 mM of each indicator in Set B (Table 1). Based on an effective  $pK_a$  value of 2,6-dimethylphenol of 10.5, the optimum pH gradient would be centred at pH 10.5 and span at least  $\pm 1$  units either side.  $C_o$  for this sample is calculated as 16 mM;  $MPA^{2-}$  is discounted from the summation as it is too weak a base to deprotonate  $HCO_3^-$ .  $\alpha$  was set at 1 as the  $pK_a$  of  $HCO_3^-$  is within 0.5 units of the expected  $pK_a$  of the analyte. 2.0 mg of  $NaHCO_3$  was weighed into a standard 5 mm NMR tube giving a  $\beta$  value of 5.4 and  $t_{opt}$  of 6.6 hours from Equations 6 and 8. A  $\beta$  value of 5.4 is predicted using the CurTiPot package<sup>32</sup> to give a pH of 9.3 at  $Z_b$ . Analysis of the sample over time as the gradient developed confirmed that the best gradient is indeed obtained at  $t_{opt}$  (Figure 1).

We note that as the  $NaHCO_3$  is in excess over  $C_o$  at  $Z_b$ , the pH is relatively insensitive to  $\beta$ . For example, the pH is predicted to be 9.2 and 9.4 with  $\beta$  values of 6.4 and 4.4 respectively.  $t_{opt}$  is calculated as 6.0 and 7.5 hours for  $\beta$  values of 6.4 and 4.4 respectively. Our method is thus tolerant of small errors in the weighing of the acid.

Although the best pH gradient for the determination of the analyte  $pK_a$  value is obtained at  $t_{opt}$ , acceptable pH gradients are attained  $\pm 2$  hours ( $\pm 30\%$ ) either side of  $t_{opt}$ . Minimal variation of the fitted analyte  $pK_a$  values is observed within this time interval. This observation is common to all the acid/analyte combinations studied in this work (Section 8, Supporting Information). A significant window of time therefore exists when the sample may be analysed, as permitted by spectrometer availability. This flexibility allows the method to be implemented through an automated sample changer. Samples were prepared simultaneously and left in a sample rack at ambient lab temperature for the gradients to develop. The samples were then analysed within the time window. Accurate  $pK_a$  values were obtained with all samples (Section 9, Supporting Information).

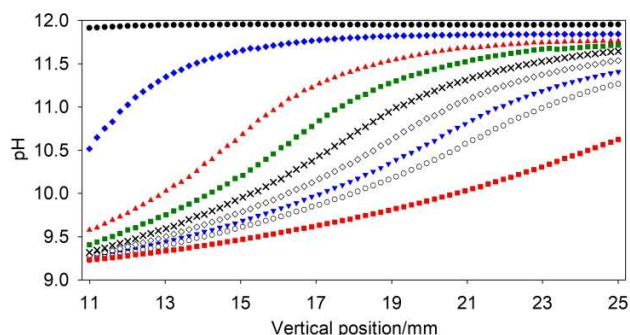


**Figure 1.** Profile of a pH gradient 0.4 hours (black circle), 2.4 (blue diamond), 4.4 (red triangle) 5.4 (green square), 6.4 (black cross;  $t_{opt} = 6.6$ ), 7.4 (white diamond), 8.4 (blue triangle), 9.4 (white circle) and 13.4 hours (red square) after sample preparation. The vertical position along the sample is as defined on the ruler on Scheme 1.

A complete set of the parameters used for all analytes is provided in Table 4. Example pH profiles obtained with each analyte are plotted on Figure 2. The pH is not plotted where it changed too rapidly with position to be measured using CSI (Section 10, Supporting Information) or where the calibration range of the indicators would be exceeded (Section 4, Supporting Information). Nevertheless, it is apparent that all pH values between 1 and 12 are accessible using the methods presented in this paper. Both the pH gradients and the analyte  $pK_a$  values obtained are highly reproducible (Section 8, Supporting Information). The measurement of a  $pK_a$  value does not require the pH gradients to be reproduced precisely. For example, minimal variation of the  $pK_a$  values is observed in samples as a function of time, despite the pH gradients changing significantly (Section 8, Supporting Information). Our *in situ* method for pH determination yields the analyte chemical shift as a function of pH, regardless of the exact shape of the gradient.

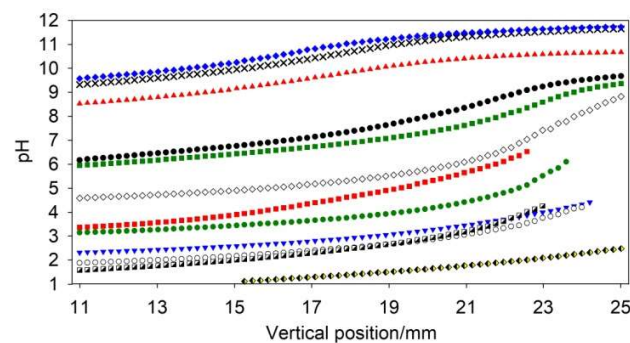


**Figure 2.** Profiles of pH gradients used to measure the analyte  $pK_a$  values: *tert*-butylamine (blue diamond), 2,6-dimethylphenol (black cross), benzylamine (red triangle), 4-cyanophenol (black circle), bromothymol blue (green square), benzimidazole (white diamond), propionic acid (malonic acid diffusant, red square; glycolic acid diffusant, green circle), glycolic acid (blue triangle), 3,5-dinitrobenzoic acid (white circle), L-tyrosine (black/white square) and 2,6-dihydroxybenzoic acid (yellow/black diamond). The vertical position along the sample is as defined on the ruler on Scheme 1.

**Table 4. Parameters used in each titration.**

Analyte	$pK_{a,Tdyn}^a$	Diffusant	I/mM <sup>b</sup>	$C_a$ /mM	$\alpha$	$\beta^c$	m/mg	$t_{opt}$ /hours <sup>c</sup>	$t_{measure}$ /hours <sup>d</sup>
<i>tert</i> -Butylamine	10.70±0.02	NaHCO <sub>3</sub>	54	16	1	5.4-5.7	2.0-2.1	6.4-6.6	6.5-6.6
2,6-Dimethylphenol	10.62±0.01	NaHCO <sub>3</sub>	55	16	1	5.4	2.0	6.6	6.4-6.6
Benzylamine	9.41±0.01	B(OH) <sub>3</sub>	16	6	1	6.7-7.4	0.7-0.8	4.7-4.9	5.0-5.9
4-Cyanophenol	8.00±0.01	KH <sub>2</sub> PO <sub>4</sub>	27	5	1	6.7-7.2	1.3-1.4	7.8-8.1	7.6-8.3
Bromothymol Blue	7.47±0.01	KH <sub>2</sub> PO <sub>4</sub>	24	5	1	6.7-8.0	1.3-1.6	7.4-8.1	8.2-9.2
Benzimidazole	5.52±0.01	NaMal	28	7	1	5.8-6.1	1.4-1.5	6.7-7.0	6.4-7.5
Propionic acid	4.78±0.02	Malonic acid	19	9	0.5	1.7-2.4	0.4-0.6	8.4-11.1	9.6-10.5
Propionic acid	4.78±0.01	Glycolic acid	17	7	1	4.9-5.5	0.7-0.8	7.1-7.7	7.0-7.5
Glycolic acid	3.76±0.01	Oxalic acid	20	13	0.5	1.7-1.9	0.7-0.8	7.6-8.5	7.9-8.5
3,5-Dinitrobenzoic acid	2.79±0.01	Oxalic acid	20	17	0.5	2.1-2.3	1.2-1.3	6.6-7.1	7.1-7.2
L-Tyrosine	2.19±0.01	Oxalic acid	24	17	0.5	4.1-4.2	2.6-2.7	4.8	4.9-5.6
2,6-Dihydroxybenzoic acid <sup>e</sup>	1.26±0.01	HCl	70	67	1	3.4	(30 $\mu$ L, 2 M)	3.2	2.7-3.1

<sup>a</sup>Average of at least three samples  $\pm$  the standard deviation. <sup>b</sup>Ionic strength at the midpoint of the titration ( $Z_a$ ) estimated using the CurTiPot package.<sup>32</sup> <sup>c</sup> $\beta$  is adjusted according to the mass of acid used in each experiment.  $t_{opt}$  is recalculated accordingly. <sup>d</sup>The time elapsed between the preparation of the sample and the recording of the NMR image. The time quoted corresponds to the midpoint of the NMR experiment. <sup>e</sup> $C_o$  for 2,6-dihydroxybenzoic acid was calculated as the sum of the concentrations of the basic species in solution (17 mM) and the free acid required to obtain a pH of approximately 1.3 (50 mM) at  $Z_a$ .

**Determination of analyte  $pK_a$  values.** By applying the methods discussed in the previous sections, smooth pH gradients and titration curves can be acquired for a range of analytes (Scheme 1, c). A complete set of titration curves for all analytes is provided in the Supporting Information (Section 12). The effective  $pK_a$  values of the analytes obtained must be extrapolated to infinite dilution to obtain the thermodynamic  $pK_a$  values,  $pK_{a,Tdyn}$ , for comparison with literature values. This can be accomplished using Equation 9:<sup>39,41,42,49,50</sup>

$$pK_{a,Tdyn} = pK_a - (z_H^2 - z_L^2) \left( 0.509 \frac{\sqrt{I}}{1 + \sqrt{I}} - 0.11 \right) \quad (9)$$

where  $I$  is the ionic strength of the solution and  $z_H$  and  $z_L$  are the charges of the protonated and deprotonated analyte species respectively. The activity coefficients of neutral or zwitterionic species are assumed to be unity.<sup>49,51</sup>

When using acid diffusants that are neutral in their protonated state (e.g. boric acid, malonic acid), the ionic strength is essentially constant throughout the titration (Table S-20, Supporting Information). However, when the acid bears a charge in its protonated state (e.g. NaHCO<sub>3</sub>, KH<sub>2</sub>PO<sub>4</sub>), the ionic strength is variable. Different approaches to correct for this variation are reviewed in the Supporting Information, Section 11. Briefly, a simple approach is to calculate the ionic strength at the midpoint ( $Z_a$ ) of the titration (Table 4) as the measured  $pK_a$  of the analyte is most sensitive to ionic strength when  $pH \approx pK_a$ .<sup>10,28</sup> The effective  $pK_a$  obtained by fitting the titration data to Equation 1 may be converted to  $pK_{a,Tdyn}$  using Equation 9. Alternatively, the concentration of acid along the gradient, and therefore the ionic strength, may be calculated using

Equation 8. Each data point in the titration may be corrected for the variation of both the indicator and analyte  $pK_a$  values with ionic strength using Equation 9.  $pK_{a,Tdyn}$  may be obtained directly by fitting. Nevertheless, no significant differences in the analyte  $pK_{a,Tdyn}$  values are obtained with these two methods (Table S-22, Supporting Information). The simpler method utilising a single-point ionic strength correction is therefore used as standard throughout this work.

The thermodynamic  $pK_a$  values of the analytes obtained agree with literature values to within  $\pm 0.1$  units. A plot of the values obtained in this work versus literature data is presented in Section 13 in the Supporting Information along with a tabulated comparison. An  $R^2$  value of 0.9999 is obtained along with a slope and intercept of 1.01 and -0.06 respectively. An accuracy of  $\pm 0.1$  units is comparable to that obtained by other methods<sup>52</sup> including capillary electrophoresis,<sup>53</sup> potentiometric titrations,<sup>38,54</sup> conductometry,<sup>51,55,56</sup> UV spectroscopy<sup>57,58</sup> and conventional NMR titrations.<sup>12,21</sup> From Equation 2, the method for the determination of pH by <sup>1</sup>H NMR may also be assumed accurate to  $\pm 0.1$  units. We note that the analyte  $pK_a$  value obtained is independent of the resonance examined (Section 12, Supporting Information).

## CONCLUSIONS

Chemical shift imaging in the presence of a controlled pH gradient allows efficient determination of precise  $pK_a$  values for analytes present in solution. The approach affords significant advantages over conventional NMR-based titration methods in terms of the quantity of sample, sample preparation time and instrument time required. The method is robust to minor variations in sample preparation. For all analytes tested,

it is possible to treat the limiting chemical shifts of the analyte as free parameters while fitting titration data to extract the  $pK_a$  value. The method is non-destructive and other information contained within the NMR spectrum is accessible suggesting the method can be extended to study other concentration dependent phenomena. For example, the  $Ca^{2+}$  triggered formation of a supramolecular gel can be monitored by measuring residual dipolar and quadrupolar couplings of small organic molecules as a function of a  $Ca^{2+}$  gradient.<sup>26</sup>

## ASSOCIATED CONTENT

Supporting information available as noted in the text.

## AUTHOR INFORMATION

### Corresponding Author

\* iggo@liverpool.ac.uk; matthew.wallace@uea.ac.uk

### Present Addresses

‡School of Pharmacy, University of East Anglia, Norwich Research Park, Norwich, NR4 7TJ, UK

#School of Chemistry, College of Science and Engineering, University of Glasgow, Glasgow, G12 8QQ, UK

### Author Contributions

All authors have given approval to the final version of the manuscript.

### Notes

The authors declare no competing financial interest.

## ACKNOWLEDGEMENTS

We thank Unilever for a Case Award (MW) and the EPSRC for funding a DTA (MW). We thank the EPSRC for funding (EP/C005643/1 and EP/K039687/1). DJA thanks the EPSRC for a Fellowship (EP/L021978/1). MW thanks the Royal Commission for the Exhibition of 1851 for a Research Fellowship.

## REFERENCES

- Han, J.; Burgess, K. *Chem. Rev.* **2010**, *110*, 2709-2728.
- Lauber, C. L.; Hamady, M.; Knight, R.; Fierer, N. *Appl. Environ. Microbiol.* **2009**, *75*, 5111-5120.
- Kishino, T.; Kobayashi, K. *Water Res.* **1995**, *29*, 431-442.
- Young, J. A. T.; Collier, R. J. *Annu. Rev. Biochem.* **2007**, *76*, 243-265.
- Sakurai, K.; Goto, Y. *Proc. Natl. Acad. Sci. U. S. A.* **2007**, *104*, 15346-15351.
- Beer, P. D.; Gale, P. A. *Angew. Chem. Int. Ed.* **2001**, *40*, 486-516.
- Du, X.; Zhou, J.; Shi, J.; Xu, B. *Chem. Rev.* **2015**, *115*, 13165-13307.
- Morris, K. L.; Chen, L.; Raeburn, J.; Sellick, O. R.; Cotanda, P.; Paul, A.; Griffiths, P. C.; King, S. M.; O'Reilly, R. K.; Serpell, L. C.; Adams, D. J. *Nat. Commun.* **2013**, *4*.
- Aggeli, A.; Bell, M.; Carrick, L. M.; Fishwick, C. W. G.; Harding, R.; Mawer, P. J.; Radford, S. E.; Strong, A. E.; Boden, N. *J. Am. Chem. Soc.* **2003**, *125*, 9619-9628.
- Ackerman, J. J. H.; Soto, G. E.; Spees, W. M.; Zhu, Z.; Evehloch, J. L. *Magn. Reson. Med.* **1996**, *36*, 674-683.
- Platzer, G.; Okon, M.; McIntosh, L. P. *J. Biomol. NMR* **2014**, *60*, 109-129.
- Bezençon, J.; Wittwer, M. B.; Cutting, B.; Smieško, M.; Wagner, B.; Kansy, M.; Ernst, B. *J. Pharm. Biomed. Anal.* **2014**, *93*, 147-155.
- Tredwell, G. D.; Bundy, J. G.; De Iorio, M.; Ebbels, T. M. D. *Metabolomics* **2016**, *12*, 152.
- Lin, R.; Yip, J. H. K.; Zhang, K.; Lip, L. K.; Wong, K. Y.; Kam, P. H. *J. Am. Chem. Soc.* **2004**, *126*, 15852-15869.
- Thordarson, P. *Chem. Soc. Rev.* **2011**, *40*, 1305-1323.
- Gunnlaugsson, T.; Glynn, M.; Tocci, G. M.; Kruger, P. E.; Pfeffer, F. M. *Coord. Chem. Rev.* **2006**, *250*, 3094-3117.
- Wallace, M.; Iggo, J. A.; Adams, D. J. *Soft Matter* **2015**, *11*, 7739-7747.
- Narain, R.; Armes, S. P. *Biomacromolecules* **2003**, *4*, 1746-1758.
- Pastor, A.; Martínez-Viviente, E. *Coord. Chem. Rev.* **2008**, *252*, 2314-2345.
- Orgován, G.; Noszál, B. *J. Pharm. Biomed. Anal.* **2011**, *54*, 958-964.
- Szakács, Z.; Hägele, G.; Tyka, R. *Anal. Chim. Acta.* **2004**, *522*, 247-258.
- Fitch, C. A.; Platzer, G.; Okon, M.; Garcia-Moreno, B. E.; McIntosh, L. P. *Protein Sci.* **2015**, *24*, 752-761.
- Lintner, K.; Femandjian, S.; St. Pierre, S.; Regoli, D. *Biochem. Biophys. Res. Commun.* **1979**, *91*, 803-811.
- Muroga, Y.; Nakaya, A.; Inoue, A.; Itoh, D.; Abiru, M.; Wada, K.; Takada, M.; Ikake, H.; Shimizu, S. *Biopolymers* **2016**, *105*, 191-198.
- Niklas, T.; Stalke, D.; John, M. *Chem. Commun.* **2015**, *51*, 1275-1277.
- Wallace, M.; Iggo, J. A.; Adams, D. J. *Soft Matter* **2017**, *13*, 1716-1727.
- Mitrev, Y.; Simova, S.; Jeannerat, D. *Chem. Commun.* **2016**, *52*, 5418-5420.
- Tynkkynen, T.; Tiainen, M.; Soininen, P.; Laatikainen, R. *Anal. Chim. Acta.* **2009**, *648*, 105-112.
- Baryshnikova, O. K.; Williams, T. C.; Sykes, B. D. *J. Biomol. NMR* **2008**, *41*, 5-7.
- Valcour, A.; Woodworth, R. C. *J. Magn. Reson.* **1986**, *66*, 536-541.
- Li, T.; Liao, Y.; Jiang, X.; Mu, D.; Hou, X.; Zhang, C.; Deng, P. *Talanta* **2018**, *178*, 538-544.
- Gutz, I. G. R.; CurTiPot - pH and Acid-Base Titration Curves: Analysis and Simulation freeware, version 4.2: ([http://www.iq.usp.br/gutz/Curtipot\\_.html](http://www.iq.usp.br/gutz/Curtipot_.html)).
- Trigo-Mouriño, P.; Merle, C.; Koos, M. R. M.; Luy, B.; Gil, R. R. *Chem. Eur. J.* **2013**, *19*, 7013-7019.
- Liu, M.; Mao, X. A.; Ye, C.; Huang, H.; Nicholson, J. K.; Lindon, J. C. *J. Magn. Reson.* **1998**, *132*, 125-129.
- Popov, K.; Rönkkömäki, H.; Lajunen, L. H. *J. Pure. Appl. Chem.* **2006**, *78*, 663-675.
- Brown, A. M. *Comput. Methods Programs Biomed.* **2001**, *65*, 191-200.
- Sigel, H.; Zuberbühler, A. D.; Yamauchi, O. *Anal. Chim. Acta.* **1991**, *255*, 63-72.
- Irving, H. M.; Miles, M. G.; Pettit, L. D. *Anal. Chim. Acta.* **1967**, *38*, 475-488.
- Daniele, P. G.; Rigano, C.; Sammartano, S. *Talanta* **1983**, *30*, 81-87.
- Capone, S.; de Robertis, A.; de Stefano, C.; Sammartano, S.; Scarcella, R.; Rigano, C. *Thermochim Acta* **1985**, *86*, 273-280.
- Davies, C. W. *J. Chem. Soc.* **1938**, 2093-2098.
- Harned, H. S.; Owen, B. B. *J. Am. Chem. Soc.* **1930**, *52*, 5079-5091.
- Crofts, P. C.; Kosolapoff, G. M. *J. Am. Chem. Soc.* **1953**, *75*, 3379-3383.
- Sigel, H.; Da Costa, C. P.; Song, B.; Carloni, P.; Gregaň, F. *J. Am. Chem. Soc.* **1999**, *121*, 6248-6257.
- King, J. F.; Hillhouse, J. H.; Skonieczny, S. *Can. J. Chem.* **1984**, *62*, 1977-1995.
- Angkawijaya, A. E.; Fazary, A. E.; Ismadji, S.; Ju, Y. H. *J. Chem. Eng. Data* **2012**, *57*, 3443-3451.
- Haynes, W. M.; ed. *CRC Handbook of Chemistry and Physics*, 95th ed.; CRC Press: Boca Raton, FL, 2014.
- Crank, J. *The Mathematics of Diffusion*, 2nd ed.; Clarendon Press: Oxford, 1975.

- (49) Nagai, H.; Kuwabara, K.; Carta, G. *J. Chem. Eng. Data* **2008**, *53*, 619-627.
- (50) Baker, M. E. J.; Narayanaswamy, R. *Sens Actuators, B Chem* **1995**, *29*, 368-373.
- (51) Belcher, D. *J. Am. Chem. Soc.* **1938**, *60*, 2744-2747.
- (52) Reijenga, J.; van Hoof, A.; van Loon, A.; Teunissen, B. *Anal. Chem. Insights* **2013**, *8*, 53-71.
- (53) Poole, S. K.; Patel, S.; Dehring, K.; Workman, H.; Poole, C. *F. J. Chromatogr. A* **2004**, *1037*, 445-454.
- (54) Qiang, Z.; Adams, C. *Water Res.* **2004**, *38*, 2874-2890.
- (55) Papadopoulos, N.; Avranas, A. *J. Solution Chem.* **1991**, *20*, 293-300.
- (56) Apelblat, A. *J. Mol. Liq.* **2002**, *95*, 99-145.
- (57) Box, K.; Bevan, C.; Comer, J.; Hill, A.; Allen, R.; Reynolds, D. *Anal. Chem.* **2003**, *75*, 883-892.
- (58) Herington, E. F. G.; Kynaston, W. *Trans. Faraday Soc.* **1957**, *53*, 138-142.



For TOC only

